Enhanced brain-derived neurotrophic factor distribution in differentiated human neuroblastoma SH-SY5Y cells by PEG-ylated protein nanoparticles: model of application in neurodegenerative diseases

Maria Dąbkowska (maria.dabkowska@pum.edu.pl)
Pomeranian Medical University https://orcid.org/0000-0003-0190-1292
Karolina Łuczkowska
Pomorski Uniwersytet Medyczny w Szczecinie
Dorota Rogińska
Pomorski Uniwersytet Medyczny w Szczecinie
Anna Sobuś
Pomorski Uniwersytet Medyczny w Szczecinie
Monika Wasilewska
Polska Akademia Nauk Instytut Katalizy i Fizykochemii Powierzchni
Zofia Ulańczyk
Pomorski Uniwersytet Medyczny w Szczecinie
Bogusław Machaliński
Pomorski Uniwersytet Medyczny w Szczecinie

Research

Keywords: Brain-derived neurotrophic factor, neurons, neurodegenerative disorders treatment, BDNF-based electrostatic complex

Posted Date: March 26th, 2020

DOI: https://doi.org/10.21203/rs.3.rs-18860/v1

Version of Record: A version of this preprint was published on August 31st, 2020. See the published version at https://doi.org/10.1186/s12951-020-00673-8.

Abstract

Brain-derived neurotrophic factor (BDNF) is essential for the development and function of human neurons, therefore it is a promising target for neurodegenerative disorders treatment. Here, we studied BDNF-based electrostatic complex with dendrimer nanoparticles encapsulated in polyethylene glycol (PEG) in injured, differentiated neuroblastoma SH-SY5Y cells, a model of neurodegenerative mechanisms. PEG layer was adsorbed at dendrimer-protein core nanoparticles to decrease their cellular uptake and to reduce BDNF-serum proteins interaction for prolonged time. Cytotoxicity and confocal microscopy analysis revealed PEG-ylated BDNF-dendrimer nanoparticles can be used for continuous neurotrophic factor delivery enhancing its distribution into cells over 24 hours without toxic effect. We offer reliable electrostatic route for efficient encapsulation and controlled transport of fragile therapeutic proteins without any covalent cross-linker; this could be considered as safe drug delivery system. Understanding of polyvalent BDNF interactions with dendrimer core nanoparticles offers new possibilities for design of well-ordered protein drug delivery systems.

1. Introduction

Nanostructures are a promising tool for efficient therapeutics delivery even to the difficult tissues, like brain, in which blood-brain barrier remains a fundamental challenge for drug delivery systems. Since brain-derived neurotrophic factor (BDNF) induces neuronal survival and tissue repair, it is a promising therapeutic agent for treatment of neurodegenerative diseases e.g. Alzheimer's disease in which cholinergic neurons are depleted[1]; Parkinson's disease[2] in which dopaminergic neurons of the substantia nigra are lost and amyotrophic lateral sclerosis[3] (ALS) in which cerebral and spinal motor neurons degenerate. However, efficient BDNF delivery to the brain poses a few difficulties.

BDNF is the most abundant member of neurotrophic factors family in the mammalian central nervous system. BDNF homodimer has about 27 kDa, exerts biological activity in a dimeric state and has a common structural motif consisting of 120 amino acids and forms three disulfide bridges. The isoelectric point of fatty acid free BDNF is pH 10-10.9. The electric charge over BDNF molecules is heterogeneously distributed. As a result, the amino acids structural elements of BDNF molecule like Lysine 96, Arginine 97, Glutamine 84 are presented in the active site, which gives the largest positively charged region over protein molecules.[4, 5] BDNF binds with high affinity to tyrosine kinase B receptor to promote trophic signaling and apoptotic events.[6-8] Indeed, low BDNF levels are observed in brains of patients suffering from multiple pathologies of central nervous system and changes in BDNF concentration or its distribution have been linked with several neurodegenerative and psychiatric disorders, like depression and schizophrenia.[9, 10]

Neurotrophins are challenging candidates for drug development, because of their low bioavailability for therapeutic targets and insubstantial pharmacokinetic behavior. Synthesis, secreted concentration and half-life of BDNF in human body are limited.[11] BDNF is the diffusible factor secreted by neuronal development system and is not available for all neurons; therefore, its delivery from cells to tissues

results in concentration gradients.[12] Accordingly, improved administration of exogenous BDNF and consequent neuroprotection as well as neuroregeneration have been considered potentially novel treatments for neurodegenerative diseases, including Parkinson disease. However, carrier-free administration of BDNF is relatively unstable because of rapid degradation in biological medium due to very short *in vivo* half-life (<2min) and low biodistribution that cause this side effect. The rational design of BDNF-based nanoparticles requires a good understanding of their interactions for controlled protein release in order to achieve higher delivery efficiency due to increased BDNF presence in the tissue as well as its improved bioavailability.

Nanocarriers such as dendrimer have been extensively studied in various BDNF drug delivery systems[13, 14] to improve their therapeutic efficiency by increasing circulation time and bioavailability at the targeted site (dendrimers possess high biocompatibility and facile functionalization lead to responsiveness to specific stimuli). In our previous studies, on 7th day post application we observed improved administration of neurotrophin-4 using dendrimer nanoparticles in impaired retina tissue.[15] Physicochemical properties of densely branched dendrimer molecules with well-defined spherical geometry, enhance stability and surface functionality of neurotrophin delivery system. Size of dendrimers nanoparticles due to their higher curvature will have a fewer number of nanoparticles ligands that can interact with protein side chains. As the result, PAMAM surface area accessible to the neurothrophin will be lower, this could potentially result in less proteins denaturation. Dendrimers present strong ability to escape from the uptake by non-specific ReticuloEndothelial System and consequently avoid long term toxicities effect[16-19]. In a localized manner, dendrimers, due to high degree of structural control (monodispersity and tunable chemical structure), can be administrated *in vivo* as a widely utilized biological functional nanocarriers for drug,[20, 21] biomacromolecule, gene delivery,[22-24] imagining agents,[25, 26] and diagnostic product.[27] The polyvalent interaction of dendrimers with protein[28, 29] resembles a common type of interaction between biological entities such as receptors and ligands or virus and cell surface, etc.[30-33] Nano-sized carriers systems with dendrimer core are monodisperse therapeutic scaffolds that would possibly allow BDNF delivery to damaged cells, enhancing its local concentration and protein stability against enzymatic degradation. Therefore, we thought to use dendrimers to improve the extracellular retaining of BDNF without the need of covalent chemistry. However, we decided to improve delivery system with PEG (poly(ethylene glycol)), what allows them prevent unspecific protein adsorption onto the nanoparticle's surface[34-36] as well as increasing in vivo blood circulation retention times. Protein resistant PEG layer is independent of the particular choice of PEG molecular weight and thicker polymer brush does not allow proteins to experience electrostatic and van der Waals attractions. PEG brushes are grafted onto dendrimer-protein surface to render them more biocompatible by making nanoparticles less visible to phagocytic cells and improving circulating half-life of nanocarriers. The overall size of negatively charged poly(amidoamine) (PAMAM) dendrimer 5.5 generation nanocarriers with PEG core could enable efficient diffusion of BDNF across the tissue.

The main goal of our study was to determine efficient encapsulation of BDNF by PAMAM nanoparticles as well as PEG-ylated -PAMAM drug delivery system and assess their usefulness in *in vitro* system using

neuroblastoma model. Therefore, the present study was designed to: (a) elucidate the BDNF desorption from well-characterized PEG-ylated PAMAM dendrimer nanoparticles, (b) investigate diffusion and cytotoxicity of PEG-ylated BDNF-PAMAM dendrimer electrostatic complex in differentiated neuroblastoma SH-SY5Y cells in real-time up to 24 hours after administration. We used this particular cell line[37-40] as a model for the degradation of dopaminergic neuron network in the *substantia nigra parts compacta* (SCs) observed in Parkinson's disease (PD) patients.[41]

2. Materials And Methods

Adsorption/desorption transition of BDNF molecules at/from PAMAM dendrimers (Figure 1) was studied in PBS buffer using the dynamic light scattering, electrophoresis, solution depletion techniques, enzyme-linked immunosorbent assay and atomic force microscopy. This allowed us to precisely determine maximum loading of BDNF molecule at PAMAM-based nanoparticles under *in situ* conditions. Afterwards, we compared desorption kinetics of BDNF from PAMAM-based nanoparticles as well as PEG-ylated -PAMAM nanoparticles in PBS buffer and in neuron-like differentiated SH-SY5Y cells environment to quantitatively assess in real time cellular internalization by neuroblastoma cells PAMAM-based nanoparticles (using spectrofluorimetry and confocal microscopy evaluation).

2.1. Nanoparticles Synthesis

BDNF:

Filtered (centrifree ultrafiltration device, Merck Group, Darmstadt, Germany) stock solutions of carrier free recombinant human BDNF (248-N4-250/CF, R&D Systems, Canada) of known concentrations (typically 250 mg L^{-1}) in the phosphate buffered saline (PBS) pH 7.4 +/- 0.2 (Biomed, Lublin, Poland) were prepared to remove aggregates and provide constant, free form protein molecules concentration in the solvent. To minimize errors in concentration measurements, two complementary spectrophotometric techniques were used: the BCA (protein quantification bicinchoninic acid assay, kit for low concentration, Abcam, kraj) and UV absorbance at 280 nm measured with microplate spectrophotometer (BioTek Epoch, United States). Prior to each measurement, the stock solution was diluted to a desired bulk concentration, typically 0.01-2 mg L^{-1}. The exact concentration of these solutions after membrane filtration was determined by commercially available ELISA assay (DY992, DY990, DY994, DY999, DY995, WA126, DY006, DY268, R&D Systems). The temperature of experiments was kept at a constant value equal to 298 ± 0.1K.

PAMAM:

The suspension of PAMAM G5.5 ethylenediamine core five and a half generation dendrimers with sodium carboxylate surface groups, (536784, Sigma Aldrich, kraj) was used as colloid carrier for BDNF. The stock suspension was diluted prior to each adsorption experiment to a desired mass concentration, equal to 10 mg L^{-1}.

PAMAM-AF488 Conjugates:

For detection of protein – PAMAM nanoparticles in differentiated neuroblastoma SH-SY5Y cells by confocal microscopy, a detectable fluorescent molecule i.e. PAMAM-AF488 was needed. We used Alexa Fluor 488Ò (AF 488)-NHS esters (Invitrogen^{TM}, kraj) ester as fluorescent label. PAMAM at 5 mg ml-1 in pH 8.0 sodium bicarbonate buffer reacted with 1 mg ml-1 amine reactive dye dissolved in dimethylformamide as described in the manufacturer's protocol, to give fluorescently labeled PAMAM-AF488 conjugates. These conjugates were purified by extensive dialysis against pH 7.4 to remove unreacted label. After dialysis, we further purified conjugates through centrifugal filtration until filtrate absorbance at 490 nm reached background levels.

BDNF-PAMAM dendrimer nanoparticles:

BDNF adsorption at PAMAM dendrimers was performed employing electrostatic interactions according to the following procedure: (1) the reference electrophoretic mobility of bare PAMAM nanoparticles was measured, (2) BDNF layers were formed by mixing equal volumes of its solutions of the bulk concentration (varied between 0.002 – 0.4 mg L^{-1}), with nanoparticle suspension of the bulk concentration 20 mg L^{-1}, (3) the electrophoretic mobility of BDNF-PAMAM nanoparticles was measured and the corresponding zeta potential was calculated. Experiments were performed at 7.4 pH, ionic strength 0.15M, 20^{o}C temperature. In all cases, for adsorption time 2000 seconds BDNF should be irreversibly adsorbed onto the surface creating monolayer as a result of short-range electrostatic interaction between BDNF and PAMAM, since the adsorption process is mediated by electrostatic interactions. The time scale for formation of additional layers is much longer than that of monolayer formation. The adsorption time of BDNF at PAMAM dendrimers was prolonged up to 6 hours in the primary adsorption experiments. To determine unbounded protein concentration after adsorption, we performed ultrafiltration with a 50kDa cutoff membrane (Millipore, Billerica, MA, USA), allowing the separation of BDNF-PAMAM (more than 80kDa) complex and BDNF molecule (28kDa). Protein concentrations were determined using ELISA protein assay.

PEG-ylated BDNF-PAMAM dendrimer nanoparticles:

Poly(ethyleneglycol) with molecular weight 4 kDa, (1546569, Sigma Aldrich) was used for encapsulation of BDNF-PAMAM dendrimer nanoparticles. PEG chains were conjugated to the nanoparticle surfaces via amide bonds formation between PEG amino groups and PAMAM carboxyl groups. An equal volume of before prepared BDNF-PAMAM and PEG (50 mg L^{-1}, pH 7.4, 0.15M PBS) solutions was stirred at room temperature for 1 h. Further, PEG-ylated BDNF-PAMAM solution was ultrafiltered with membrane 10 kDa cutoff (Millipore, Amicon) to remove unconjugated PEG chains.

2.2. Determination of nanoparticle size distribution

– bulk

For size determination of BDNF, PAMAM 5.5, BDNF-PAMAM and PEG-ylated BDNF-PAMAM, a dynamic light scattering (DLS) was used.

Suspensions of nanoparticles as well as protein diluted with 0.15M PBS buffer to a suitable concentration were measured in Zetasizer Nano ZS apparatus (Malvern Instruments, Malvern, UK) equipped with a laser of 633nm wavelengths. Data analysis was performed in automatic mode at 25°C. Measured size was presented as the average value of 20 runs, with triplicate measurements within each run. Particle size distributions were obtained from measured diffusion coefficients.

-surface

Ruby muscovite mica (Continental Trade, Poland) was used as a substrate for BDNF, PAMAM and BDNF based nanoparticles, adsorption measurements. Fresh, solid pieces of mica were cleaved into thin sheets prior to every experiment.

The AFM (atomic force microscopy) technique was used to obtain information about the size distribution of BDNF, PAMAM dendrimers and nanoparticles. The nanoparticle as well as BDNF protein were left to deposit on mica sheets placed in the diffusion cell over a controlled time, and then substrate was removed, rinsed for half an hour in ultrapure water. The samples were left for air-drying until the next day. Next, the dry sample was placed under 7-10 nm AFM tip. The AFM measurements were carried out under ambient air conditions using the NanoWizard AFM (JPK Instruments AG, kraj). The intermittent contact mode images were obtained in the air, using ultrasharp silicon cantilevers (NSC35/AlBS, MicroMash, Spain) and the cone angle of the tip was less than 20°. The images were recorded at the scan rate of 1 Hz for the six randomly chosen places. The images were flattened using an algorithm provided with the instrument. We captured all images in random areas within the scan size of 0.5 x 0.5 μm or 1 x 1 μm. BDNF, PAMAM 5.5, BDNF-PAMAM and PEG-ylated BDNF-PAMAM surface dimensions were determined using ImageJ software by gathering the number and coordinates of single protein/nanoparticles molecules. Manual counting of protein/nanoparticles molecules was based on comparing the original image and the same picture altered by digital image filters by cutting off the picture background.

2.3. Nanoparticle zeta potential determination

The electrophoretic mobility of BDNF molecules, PAMAM, BDNF-PAMAM as well as PEG-ylated BDNF-PAMAM nanoparticles was measured at pH 7.4 and 0.15M ionic strength with Laser Doppler Velocimetry (LDV) technique with the aid of the abovementioned Malvern device. Electrophoretic mobility was recalculated to zeta potential using Henry equation valid for higher ionic strength where the polarization of the electric double layer is relevant (the double-layer thickness becomes smaller than the protein dimension).

2.4. Cell culture and differentiation

SH-SY5Y neuroblastoma cells (human, ECACC; Sigma Aldrich, St. Louis, MO, USA) were used in this study. SH-SY5Y cells were incubated in culture plates in proliferation medium containing Ham's F-12 Nutrient Mixture (Thermo Fisher, Waltham, MA, USA) and minimum essential medium (MEM) (Sigma Aldrich, St.Louis, MO, USA) mixed in ratio 1:1 and supplemented with streptomycin (100 μg/mL),

penicillin (100 U/mL), L-glutamine (2 mM) and 15% heat-inactivated fetal bovine serum (FBS) at 37◦C in saturated humidity atmosphere containing 5% CO_2. The proliferation medium was changed every 2-3 days, and the cells were passaged when they reached 80% confluence. After the proliferation step, the cells were transferred into new culture plates and incubated 24h with MEM supplemented with penicillin (100 U/mL), streptomycin (100 µg/mL), L-glutamine (2mM) and 1% FBS. On the next day, the medium was changed to a differentiation medium consisting of MEM supplemented with penicillin (100 U/mL), streptomycin (100 µg/mL), L-glutamine (2mM), 1% FBS and *Retinoic* Acid (0.01µmol/mL) (RA, Sigma Aldrich, St.Louis, MO, USA). The differentiation was carried out for 5 days and the medium was changed every 2 days.

2.5. Nanoparticles Cytotoxicity

Differentiated SH-SY5Y cells were incubated at a density of $3x10^4$ cells/well in 96-well plates for 24h with MEM (without FBS) containing 6-Hydroxydopamine (0.1µmol/mL) (6OHD, Sigma Aldrich, St.Louis, MO, USA). Then the cells were incubated for 24h with different concentration of BDNF, BDNF-PAMAM dendrimer nanoparticles or PEG-ylated BDNF-PAMAM dendrimer nanoparticles, adding 20µl to each well of selected solution prepared in PBS (described in 2.1. Nanoparticles Synthesis) and 80µl MEM without FBS. The last step was to measure toxicity using the MTT assay (Abcam, Cambridge, UK), which protocol is based on the conversion of water soluble 3-(4,5-dimethylthiazol-2-yl)-2,5-diphenyltetrazolium bromide to an insoluble formazan product, which has a purple color. Cells were incubated with 50 µL of MTT reagent mixed with 50µl MEM for 3h, then 150µl of detergent solution was added to solubilize the colored crystals. Finally, absorbance was measured at OD590nm using Varioskan LUX Multimode Microplate Reader (Thermo Fisher, Waltham, MA, USA). Toxicity was calculated from the equation in the manufacturer's protocol.

2.6. BDNF Quantification

- in PBS

The protein release kinetics from PAMAM as well as PEG-ylated PAMAM nanoparticles was assessed by using ultrafiltration method with a 30kDa cutoff membrane (Millipore, Billerica, MA, USA) in PBS at pH 7.4 and 0.15M ionic strength. It was done in two-stage procedure, where first BDNF adsorption process was carried out for 1 hour. The BDNF molecules released from nanoparticles were quantified with ELISA immunoassay method according to the manufacturer’s protocol. Initially, the residual (unbound) BDNF concentration in the filtrate was determined immediately after adsorption at PAMAM nanoparticles by applying sandwich ELISA technique to monitor simultaneously the maximum concentration of unbound BDNF in the supernatant suspensions. Thus, it was possible to precisely determine concentration of non-adsorbed BDNF molecules at PAMAM as well as PEG-ylated PAMAM nanoparticle surface. These measurements were utilized for determining the maximum coverage of neurotrophin under various protein bulk condition (0.002-1 mg L^{-1}). Afterward, the concentration of desorbed BDNF for different time

increment (20 min, 2h, 3h, 5h, 8h, 10h, 24h) was quantified by UV-VIS spectroscopy and calculated according to ELISA standard curve.

- in neuroblastoma cell culture

Concentration of releasing BDNF molecules was determined by exposing differentiated human neuroblastoma cells SH-SY5Y to 6-hydroxydopamine (6-OHDA) as well as nanoparticles with different BDNF concentrations for 24h at 37 ^{o}C. At the end of the treatments /incubation, the medium was discarded and collected to quantify BDNF concentration using UV-VIS spectroscopy calculated according to ELISA standard curve.

2.6. Internalization of PAMAM-based nanoparticles

In addition, the cellular internalization of nanoparticles with BDNF by SH-5YSY neuroblastoma cells was further investigated by determination of green fluorescence of PAMAM-AF488 conjugates. Differentiated SH-SY5Y cells and previously treated with 6OHDA (protocol described in 2.5. Nanoparticles Cytotoxicity) were incubated at a density of 3x10^4 cells/well in 96-well plates with BDNF-PAMAM-AF488 and BDNF-PAMAM-AF488-PEG nanoparticles (0.1 µg/mL protein loading) for different time lengths (2min, 5min, 10min, 30min, 1h, 4h and 24h) and were subjected to examinations by spectrofluorimetry evaluation using Varioskan LUX Multimode Microplate Reader.

2.7. Immunofluorescent labeling- nanoparticles imaging *in vitro*

For immunofluorescence analysis SH-SY5Y cells were plated in 4-well chamber slides at density 5x10^4/well. After the differentiation and 6OHD treatment (protocols described in sections 2.4 and 2.5, respectively) cells were incubated with BDNF-PAMAM-AF488 and BDNF-PAMAM-AF488-PEG nanoparticles (0.1 µg/mL protein loading) for different time lengths (5min, 10min, 30min, 1h and 24h). At designated time points, cells were washed with PBS and fixed with 70% ethanol for 15min. To visualize surface glycoproteins, cells were stained with wheat germ agglutinin conjugated to Texas Red-X (WGA-Texas Red-X, Thermo Fisher, Waltham, MA, USA) in HEPES buffer for 30min. After DAPI counterstain, the slides were mounted and subjected to z-stack analysis using a LSM700 confocal system (Carl Zeiss, Jena, Germany).

2.8. Statistical analysis

All presented data are expressed as means +/- SD from at least three independent experiments. Statistical analysis among each study group was performed using Kruskal-Wallis test. Two-Way ANOVA was used for analysis between experimental groups. $p < 0.05$ was considered statistically significant. The data are presented as the mean ± standard deviation (SD).

3. Results And Discussion

3.1 Characterization of PAMAM-based nanoparticles

PAMAM-based nanoparticles were prepared based on a modified literature method. The prepared BDNF-PAMAM as well as PEG-ylated BDNF-PAMAM nanoparticles were physicochemically characterized in terms of size, polydispersity index and electrophoretic mobility/zeta potential in 0.15M PBS buffer without calcium and magnesium ions, pH 7.4.

Dynamic light scattering analysis for BDNF-PAMAM nanoparticles revealed a mean diameter of 7.1 +/- 1.1 nm, suggested by a relatively low polydispersity index (Pdi) of less than 0.2. As shown in Figure 2a the mean hydrodynamic diameter and Pdi values obtained for BDNF-PAMAM nanoparticles were significantly lower from the PEG-ylated BDNF-PAMAM ones (10.5 +/- 1.3 nm), showing that PEG-functionalization influences the average size and polydispersity of the nanoparticles. The length of PEG in fully stretched conformation with molecular weight 4 kDa gives 32 nm in length. Results obtained from DLS clearly indicate that PEG chains are coil, fold or twist on PAMAM-BDNF surface.

The electrophoretic mobility of BDNF-PAMAM nanoparticles (suspension of the bulk concentration 10 mg L^{-1}PAMAM and 0.02-2 mg L^{-1}BDNF) obtained a negative value of -1.51 +/- 0.35 μm cm/s V to -1.72 +/- 0.19 μm cm/s V, which corresponds to a zeta potential of -19.2+/- 4.38 mV to -22 +/- 2.45 mV (calculated using the Henry relationship as described elsewhere)[42, 43] for pH 7.4; 0.15 M PBS. The zeta potential of BDNF-PAMAM-PEG nanoparticles (PEG bulk concentration is 25 mg L^{-1}) increased with adsorption of polyelectrolyte layer and reached a value of -10.7 +/- 2.2 mV, which indicates that the PEG molecule acquired a net of negative charge. The negative zeta potential values obtained for above nanoparticles were observed for unsaturated PEG layer. PEG modified the surface charge of BDNF-PAMAM nanoparticles; even though it is nominally uncharged, it reduces the number of charge groups on the PAMAM-based nanoparticles surfaces and thus affects colloidal stability.

The AFM measurements allowed us to determine the size range of nanoparticles adsorbed on mica surfaces under the diffusion-controlled transport condition at pH 7.4 and an ionic strength 0.15 M PBS.

As can be seen in Figure 3, the average PAMAM-BDNF nanoparticle occupies the equivalent of spherical area with a diameter around 7 ± 2 nm. The distribution of PAMAM-BDNF nanoparticles diameters confirms that nanoparticles exist as isolated individuals. This enables us to exactly determine their sizes by cutting down the possibility of tip convolution artifacts. According to the results from Figure 3, the size of the adsorbed single PAMAM-BDNF-PEG nanoparticle was around 11 ± 2 nm.

Moreover, colloidal stability of all PAMAM-based nanoparticles was probed by additional DLS studies. No significant size increase was found in PBS solutions of different protein concentrations, demonstrating the high colloidal stability of PEGylated BDNF-PAMAM nanoparticles. Contrary to BDNF-PAMAM nanoparticles which show noticeable agglomeration tendency, PEGylation may improve colloidal nanoparticles stability via steric repulsion, even under high salt conditions.

3.2. BDNF release from PAMAM-based nanoparticles in PBS buffer

In order to determine the possibility of desorption from dendrimers-based nanoparticles, once adsorption reached equilibrium, before the *in vitro* toxicity test was performed, we studied the BDNF release in PBS buffer.

Initially, adsorption of slightly positively charged BDNF molecules to negatively charged PAMAM dendrimers core surfaces was precisely determined to control the concentration of unbounded protein molecule and protein-laden nanoparticles structure. For every system the saturation concentration of protein has to be determined empirically. PAMAM nanoparticle is characterized with significant changes in its apparent zeta potential during adsorption, which can be efficiently monitored by LDV method. Importantly, at pH 7.4 BDNF molecule carry a net positive charge adsorb onto negatively charged uniform surface. After loading of BDNF into PAMAM-based nanoparticles, we determined the dependence of the zeta potential of nanoparticles on the initial concentration of BDNF in the PAMAM suspension (after mixing). As is depicted in Figure 1 (Supporting information), zeta potential abruptly increases with increasing BDNF concentration and approaches the plateau values of -15 mV, which is considerably below the zeta potential of BDNF molecules determined in the bulk (5mV at 0.15M ionic strength). The electrophoretic mobility of BDNF-PAMAM complex is far from value obtained for electrophoretic mobility of BDNF in the bulk (2 mg L^{-1} protein concentration), which corresponds to the formation of unsaturated neurotrophins structures on PAMAM cores.

At this point, we applied ELISA method to evaluate more accurately concentration of desorbed BDNF molecules from PAMAM as well as PEG-PAMAM nanocarriers in electrolyte solution. The release profiles of BDNF molecules from nanoparticles at various initial concentration of protein from 0.02 to 2 mg L^{-1} is shown in Fig. 4 (pH 7.4, 0.15 M PBS, adsorption time 30 min).

For both type of nanoparticles, first phase in releasing profile is characterized by a fast release of BDNF molecules from their surfaces, which probably results from the solubilization of protein adjoining dendrimer surface. In all cases, for loaded concentration of BDNF 0.02 mg L^{-1} the spontaneous electrostatic interaction led to release less than 10 ng L^{-1} of BDNF from 5 h up to 24 hours, what gives less than 0,01% of loaded protein. One can see that for BDNF concentration less than 0.02 mg L^{-1} at dendrimer surface, desorption of protein molecule was negligible, indicating that its adsorption onto 10 mg L^{-1} PAMAM nanoparticles was almost completed. In this way, we found that PAMAM molecules for laden BDNF concentration less than 0.02 mg L^{-1} are likely to form irreversibly adsorbed BDNF layer therefore effect of substrate remains significant, making the desorption process less efficient than in case of densely packed layers.

For greater protein loadings, desorption of BDNF from PEG-PAMAM nanocarriers is characterized by a sustained release of protein molecules. For BDNF desorption kinetics from PEG-PAMAM nanoparticles, it can be noted that for first 5h we observed significant desorption of protein from nanoparticle surfaces in comparison to PAMAM-BDNF nanoparticles, indicating that additional polyelectrolyte layer improved the diffusion of the weakly entrapped protein from nanoparticles surfaces. For both types of nanocarriers, for the highest concentration of laden protein used, BDNF concentration reached maximum constant value

after 10h of desorption, for PAMAM-BDNF nanoparticles and PEG-ylated PAMAM-BDNF (Fig. 4) equal to 21 ng L^{-1} and 39 ng L^{-1}, respectively. For higher protein concentration, BDNF molecules are forced to adsorb at protein previously bound to dendrimer surface, thus enhancing repulsive electrostatic interaction within the layers which causes the increase in binding energy of these molecules. These data strongly suggest that some fraction of less tightly bound BDNF molecule to PAMAM surface exists which improves penetration across the PEG layer. Abruptly desorbed fraction of reversibly bound BDNF molecules from dendrimer-based nanocarrier during the course of desorption, may indicate the existence of certain population of neurotrophin aggregates in the adsorbed state or conformational changing of single BDNF molecule during adsorption. This suggests that BDNF molecules reside within the PEG coating of the PAMAM rather than on the PAMAM surface.

Moreover, considering data obtained from ELISA and LDV measurements we noticed that irreversibility of BDNF adsorption process at dendrimers surfaces should be expected at pH significantly smaller than isoelectric point of protein, where BDNF molecules and dendrimers particles have opposite electrokinetic charge. The BDNF desorption from PAMAM surfaces was consistent with previous data obtained for another neurotrophin (NT-4) desorbed from solid surface where results were interpreted in terms of the electrokinetic model for the concentration range of 0.1-1 mg L^{-1}, postulating an irreversible adsorption of the protein governed by the random sequential adsorption.

3.3 Nanoparticle toxicity

In order to determine the possibility of the toxicity of PAMAM-based nanoparticles in biomedical applications, under increased concentration of BDNF, we examined cell viability in modified neuroblastoma SH-SY5Y cancer cells.

At the beginning we differentiated SH-SY5Y cells by combination of RA treatment and lowering FBS in cell culture according to reports[44-47]. We observed, that extension of neurites, a typical neuronal phenotype, was visible 48 h after application of retinoic acid and retained till 7 days according to Ref.[44] We observed change in SH-SY5Y cell morphology during the differentiation process, the induction of extensive neurites outgrowth as early as 48h of treatment.

Systemic administration of 6-OHDA toxin is known to selectively impair the dopaminergic neurons, resulting in cell death and selectively kills neurons in substantia nigra and striatum in animals model Ref.[48] To establish experimental dosage for testing toxicity of PAMAM-based nanoparticles, first we determined their responsiveness to 6-OHDA dose-response plot (Fig.5).

We examined differentiated SH-SY5Y cells responsiveness to various concentrations of 6-OHDA for 24h and drug neurotoxicity was assessed by MTT assay. Reduction of cell viability was employed here as an indicator of cell proliferation and toxicity. We established that exposure to 100 μMol/L 6-OHDA resulted in a significant 70% decline in cell viability. After exploring the differences in toxicity upon exposure to varying concentrations of 6-OHDA, we chose 100 μMol/L 6-OHDA for further studies and used this

concentration to determine the cytotoxicity of PAMAM-based nanoparticles with different loading BDNF concentration on differentiated SH-SY5Y cells after 24h of incubation (Fig. 6).

For neuroblastoma cell line, the critical PAMAM dendrimer concentration, above which significant decrease in cell viability (cytotoxicity) occurs is ~20 mg L^{-1} (Supporting information). The MTT assay demonstrated that no observable toxicity was detected for nanoparticles with 10 mg L^{-1} concentration of PAMAM 5.5 dendrimers. The data presented in Figure 6 further shows that after 24h of nanoparticles incubation with SH-SY5Y, the cell viability increases from initial value obtained only for BDNF without any carriers (90%) to PAMAM-based nanoparticles (150%). Less pronounced cytotoxicity in SH-SY5Y cells by PAMAM-based nanoparticles than BDNF without nanocarriers may reflect differences in the relative susceptibility of BDNF internalization. Moreover, with increasing concentration of protein loading, a decrease in toxicity was observed only for PAMAM-BDNF nanoparticles reversely to PEG-ylated one. There was a significant statistical difference between the effect of BDNF, dendrimers and PEG-ylated dendrimers nanoparticles.

A marked increase in SH-SY5Y cell viability in the presence of PAMAM-BDNF and PEG- PAMAM-BDNF nanoparticles for high protein concentration (41 and 52%, respectively), compared to the BDNF without carrier, indicates that PEG layer markedly decreased *in vitro* cellular toxicity level of employed BDNF.

3.4 Cellular uptake and imaging of PAMAM-based nanoparticles in neuroblastoma cell line SH-SY5Y

To understand whether neural-like cells are able to take up PAMAM-BDNF and PEG-PAMAM-BDNF nanoparticles we used confocal microscopy as well as spectrofluorimetry. Confocal analysis was conducted to qualitatively assess the localisation of BDNF-PAMAM-AF488 and BDNF-PAMAM-AF488-PEG nanoparticles and cellular uptake up to 24h.

As shown in Figure 7, differentiated neuron-like SH-5YSY neuroblastoma cells exhibited kinetic-dependent internalization of both types of nanoparticle. We found that from 5 min after the addition of PAMAM based nanoparticles with 0,1 mg L^{-1} BDNF concentration up to 24h, there was no observable cellular internalization likely because of inefficient endocytosis. These results were more apparent for BDNF-PAMAM-AF488-PEG nanoparticles which strongly suggest that protein molecules encapsulated in polyelectrolyte with their appropriate sizes are well protected, and effectively adsorbed by cells membrane. PEG's floppy chains and their charge neutrality can prevent non-specific adsorption and prevent or enhance linking chemistry via electrostatic repulsion or attraction, what involves nanoparticles interactions with an appropriate number of cell surface sites, which are necessary to produce an adequate binding energy.

In addition, nanoparticles with BDNF were incubated with SH-5YSY neuroblastoma cells for different time lengths (2min, 5min, 10min, 30min, 1h, 4h and 24h) and subjected to examinations by spectrofluorimetry evaluation. The cellular internalization of BDNF-PAMAM-AF488 and BDNF-PAMAM-AF488-PEG by SH-5YSY neuroblastoma cells was investigated by determination of green fluorescence intensity.

In line with the confocal microscopy results, significantly more pronounced green fluorescence was observed within the cells treated with BDNF-PAMAM-AF488, when compared to those of the cells incubated with BDNF-PAMAM-AF488-PEG. This confirms significantly hampered cellular internalization, likely because of inefficient endocytosis of nanoparticles by cells.

As shown in Figure 8, upon incubation of SH-5YSY neuroblastoma cells with BDNF-PAMAM-AF488, increase in green fluorescence was evident after 24h, in a dramatic contrast to that of 2 min-treated cells where little green fluorescence was observed, suggesting an efficient interaction with cell membrane for both type of nanoparticles. In fact, given enough time, more BDNF molecules could be released from PAMAM-based nanoparticles in immediate vicinity and subsequently enter nucleus. Cellular uptake in serum-free media is greatly reduced for PEG-ylated PAMAM-BDNF nanoparticles compared to the non-PEGy-lated.

3.5. BDNF release from PAMAM-based nanoparticles *in vitro*

The sustained delivery of proteins from dendrimer nanoparticles was determined to assess a therapeutic level of the neurotrophin over prolonged periods. We investigated the suitability of PAMAM nanoparticles to the *in vitro* transportation of BDNF to differentiated neuroblastoma cells exposed to treatment of 6-hydroxydopamine. This study was designed to quantitatively identify penetration of BDNF within damaged neuron-like cells. To assess the distribution of injected dendrimer-neurotrophin conjugates, we analyzed the BDNF concentrations after administration of BDNF and nanoparticles, using ELISA after 24 hours post-treating. The cells exposed to RA and 25μMol/L 6OHDA served as controls. The results are summarized in Figure 9.

We observed that BDNF concentration in the PAMAM-based nanoparticles-treated groups significantly increased compared to the control at 24h. Released BDNF from PAMAM based nanoparticles to extracellular region led to a significant increase in their concentration level compared to the control groups (100 μM 6OHDA) for both type of PAMAM-based nanoparticles. We found that PEG-ylated PAMAM-BDNF nanoparticles-treated cells expressed significantly higher level of neuroprotective protein when compared with the PAMAM-BDNF nanoparticles-treated group. These difference in the BDNF levels in extracellular region in the PEG-ylated PAMAM-BDNF nanoparticles-treated group compared to the PAMAM-BDNF nanoparticles-treated group are in line with releasing protein profile presented in PBS. For BDNF release kinetics from PEG-BDNF-PAMAM nanoparticles in PBS after 24h of treating, we observed significant desorption of BDNF from nanoparticle surfaces compared to PAMAM-BDNF nanoparticles of laden protein 1 mg L^{-1} and 2 mg L^{-1} equal to 39 ng L^{-1} and 42 ng L^{-1} respectively. Treating differentiated human neuroblastoma cell line SH-SY5Y with PAMAM-based nanocarriers intensifies the secretion of BDNF. These data strongly suggest that there is some interaction between surface TrkB cell receptors and BDNF nanoparticles in that system. Thus, the local secretion of BDNF may then have exerted its action locally, through its stimulatory effect on nerve regeneration acting as retrograde signal for survival neurons via the TrkB receptor. The increase in size, colloidal stability and reduction of surface charge

density for PEG-ylated nanoparticles could lead to less efficient cellular internalization by differentiated SH-SY5Y cells through hampering interactions with their TrkB receptors.

4. Conclusion

In the design of nanocarriers for neurodegenerative diseases treatment the sustained administration of neuroprotective protein is required. Therefore, in this study we introduced a versatile nanoparticles based on the use of dendrimers for BDNF delivery. Rapid cellular interaction of PAMAM dendrimers-BDNF nanoparticles with cells membrane was detected as early as 2 min, which positively affects release of therapeutic protein for damaged cells at later time points. Encapsulation of PAMAM dendrimers-BDNF nanoparticles into PEG layer further improves the design, through increasing colloidal stability and BDNF release. Increase in concentration of released BDNF in extracellular region as well as cell viability for PEG-ylated PAMAM-BDNF nanoparticles-treated group compared to the PAMAM-BDNF nanoparticles-treated group in differentiated neuroblastoma SH-SY5Y cells strongly suggest a decreased insertion of PEGylated nanoparticle into intracellular environment. PEGylated PAMAM-based nanoparticles could possibly allow us to enhance therapeutic efficacy in neuron-like cells and devise a robust procedure for preparing stable and well-controlled dendrimer-based nanoparticles.

Supporting Information

The dependence of the zeta potential of PAMAM 5.5 nanooparticles on the initial BDNF concentration in the suspension at pH 7.4, 0.15 M PBS. Determination the cytotoxicity of PAMAM 5.5 nanoparticles on 70% damaged, differentiated human neuroblastoma SH-SY5Y cells after 24h of incubation.

Declarations

Authors’ contribution

K.Ł. preparation of cell culture, D.R. confocal microscopy experiments, M.W. DLS and AFM microscopy experiments, M.D. data analyse and manuscript writing; A.S. graphics preparation

Funding

This work was supported by the National Centre for Research and Development grant STRATEGMED1/234261/2NCBR/2014.

Author information

Maria Dąbkowska, Bogusław Machaliński are co-corresponding authors

Affiliations

[1] *Department of Medical Chemistry, Pomeranian Medical University, Rybacka 1, 70-204 Szczecin, Poland.* [2] *Department of General Pathology, Pomeranian Medical University, Rybacka 1, 70-204 Szczecin, Poland.* [3] *Jerzy Haber Institute of Catalysis and Surface Chemistry Polish Academy of Sciences,Niezapominajek 8, 30-239 Cracow, Poland*

Competing interests

The authors declare no competing interests.

Consent for publication

We agree for publication.

Data availability

The data required to reproduce these findings are availability for any research.

Data availability

Acknowledgements

We thank the National Centre for Research and Development for financial support this study.

Ethics approval and consent to participate

Ethical approval and consent were not needed in this study.

References

1. Tanila, H., The role of BDNF in Alzheimer's disease. *Neurobiol Dis* **2017,** 97, (Pt B), 114-118.
2. Tome, D.; Fonseca, C. P.; Campos, F. L.; Baltazar, G., Role of Neurotrophic Factors in Parkinson's Disease. *Curr Pharm Des* **2017,** 23, (5), 809-838.
3. Baumert, B.; Sobus, A.; Golab-Janowska, M.; Ulanczyk, Z.; Paczkowska, E.; Luczkowska, K.; Zawislak, A.; Milczarek, S.; Osekowska, B.; Meller, A.; Machowska-Sempruch, K.; Welnicka, A.; Safranow, K.; Nowacki, P.; Machalinski, B., Local and Systemic Humoral Response to Autologous Lineage-Negative Cells Intrathecal Administration in ALS Patients. *Int J Mol Sci* **2020,** 21, (3).
4. Ibanez, C. F., Neurotrophic factors: from structure-function studies to designing effective therapeutics. *Trends Biotechnol* **1995,** 13, (6), 217-27.
5. Robinson, R. C.; Radziejewski, C.; Stuart, D. I.; Jones, E. Y., Structure of the brain-derived neurotrophic factor/neurotrophin 3 heterodimer. *Biochemistry* **1995,** 34, (13), 4139-46.
6. Scott-Solomon, E.; Kuruvilla, R., Mechanisms of neurotrophin trafficking via Trk receptors. *Mol Cell Neurosci* **2018,** 91, 25-33.

7. Bailey, J. J.; Kaiser, L.; Lindner, S.; Wust, M.; Thiel, A.; Soucy, J. P.; Rosa-Neto, P.; Scott, P. J. H.; Unterrainer, M.; Kaplan, D. R.; Wangler, C.; Wangler, B.; Bartenstein, P.; Bernard-Gauthier, V.; Schirrmacher, R., First-in-Human Brain Imaging of [(18)F]TRACK, a PET tracer for Tropomyosin Receptor Kinases. *ACS Chem Neurosci* **2019,** 10, (6), 2697-2702.
8. Chao, M. V., Neurotrophins and their receptors: a convergence point for many signalling pathways. *Nat Rev Neurosci* **2003,** 4, (4), 299-309.
9. Li, J.; Zhang, X.; Tang, X.; Xiao, W.; Ye, F.; Sha, W.; Jia, Q., Neurotrophic factor changes are essential for predict electroconvulsive therapy outcome in schizophrenia. *Schizophr Res* **2020**.
10. Zhou, C.; Zhong, J.; Zou, B.; Fang, L.; Chen, J.; Deng, X.; Zhang, L.; Zhao, X.; Qu, Z.; Lei, Y.; Lei, T., Meta-analyses of comparative efficacy of antidepressant medications on peripheral BDNF concentration in patients with depression. *PLoS One* **2017,** 12, (2), e0172270.
11. Atasoy, I. L.; Dursun, E.; Gezen-Ak, D.; Metin-Armagan, D.; Ozturk, M.; Yilmazer, S., Both secreted and the cellular levels of BDNF attenuated due to tau hyperphosphorylation in primary cultures of cortical neurons. *J Chem Neuroanat* **2017,** 80, 19-26.
12. Dravid, A.; Parittotokkaporn, S.; Aqrawe, Z.; O'Carroll, S. J.; Svirskis, D., Determining Neurotrophin Gradients in Vitro To Direct Axonal Outgrowth Following Spinal Cord Injury. *ACS Chem Neurosci* **2020,** 11, (2), 121-132.
13. Geral, C.; Angelova, A.; Lesieur, S., From molecular to nanotechnology strategies for delivery of neurotrophins: emphasis on brain-derived neurotrophic factor (BDNF). *Pharmaceutics* **2013,** 5, (1), 127-67.
14. Lopes, C. D. F.; Goncalves, N. P.; Gomes, C. P.; Saraiva, M. J.; Pego, A. P., BDNF gene delivery mediated by neuron-targeted nanoparticles is neuroprotective in peripheral nerve injury. *Biomaterials* **2017,** 121, 83-96.
15. Dabkowska, M.; Roginska, D.; Klos, P.; Sobus, A.; Adamczak, M.; Litwinska, Z.; Machalinska, A.; Machalinski, B., Electrostatic complex of neurotrophin 4 with dendrimer nanoparticles: controlled release of protein in vitro and in vivo. *Int J Nanomedicine* **2019,** 14, 6117-6131.
16. Stasko, N. A.; Johnson, C. B.; Schoenfisch, M. H.; Johnson, T. A.; Holmuhamedov, E. L., Cytotoxicity of polypropylenimine dendrimer conjugates on cultured endothelial cells. *Biomacromolecules* **2007,** 8, (12), 3853-9.
17. Parimi, S.; Barnes, T. J.; Callen, D. F.; Prestidge, C. A., Mechanistic insight into cell growth, internalization, and cytotoxicity of PAMAM dendrimers. *Biomacromolecules* **2010,** 11, (2), 382-9.
18. Feliu, N.; Kohonen, P.; Ji, J.; Zhang, Y.; Karlsson, H. L.; Palmberg, L.; Nystrom, A.; Fadeel, B., Next-generation sequencing reveals low-dose effects of cationic dendrimers in primary human bronchial epithelial cells. *ACS Nano* **2015,** 9, (1), 146-63.
19. McNerny, D. Q.; Leroueil, P. R.; Baker, J. R., Understanding specific and nonspecific toxicities: a requirement for the development of dendrimer-based pharmaceuticals. *Wiley Interdiscip Rev Nanomed Nanobiotechnol* **2010,** 2, (3), 249-59.

20. Li, N.; Cai, H.; Jiang, L.; Hu, J.; Bains, A.; Gong, Q.; Luo, K.; Gu, Z., Enzyme-Sensitive and Amphiphilic PEGylated Dendrimer-Paclitaxel Prodrug-Based Nanoparticles for Enhanced Stability and Anticancer Efficacy. *ACS Appl Mater Interfaces* **2017,** 9, (8), 6865-6877.
21. Iezzi, R.; Guru, B. R.; Glybina, I. V.; Mishra, M. K.; Kennedy, A.; Kannan, R. M., Dendrimer-based targeted intravitreal therapy for sustained attenuation of neuroinflammation in retinal degeneration. *Biomaterials* **2012,** 33, (3), 979-88.
22. Lamy, C. M.; Sallin, O.; Loussert, C.; Chatton, J. Y., Sodium sensing in neurons with a dendrimer-based nanoprobe. *ACS Nano* **2012,** 6, (2), 1176-87.
23. Choi, S. K.; Myc, A.; Silpe, J. E.; Sumit, M.; Wong, P. T.; McCarthy, K.; Desai, A. M.; Thomas, T. P.; Kotlyar, A.; Holl, M. M.; Orr, B. G.; Baker, J. R., Jr., Dendrimer-based multivalent vancomycin nanoplatform for targeting the drug-resistant bacterial surface. *ACS Nano* **2013,** 7, (1), 214-28.
24. Wang, F.; Zhang, B.; Zhou, L.; Shi, Y.; Li, Z.; Xia, Y.; Tian, J., Imaging Dendrimer-Grafted Graphene Oxide Mediated Anti-miR-21 Delivery With an Activatable Luciferase Reporter. *ACS Appl Mater Interfaces* **2016,** 8, (14), 9014-21.
25. Cao, J.; Ge, R.; Zhang, M.; Xia, J.; Han, S.; Lu, W.; Liang, Y.; Zhang, T.; Sun, Y., A triple modality BSA-coated dendritic nanoplatform for NIR imaging, enhanced tumor penetration and anticancer therapy. *Nanoscale* **2018,** 10, (19), 9021-9037.
26. Kim, K.; Lee, J.; Jo, G.; Shin, S.; Kim, J. B.; Jang, J. H., Dendrimer-Capped Gold Nanoparticles for Highly Reliable and Robust Surface Enhanced Raman Scattering. *ACS Appl Mater Interfaces* **2016,** 8, (31), 20379-84.
27. Ma, W.; Fu, F.; Zhu, J.; Huang, R.; Zhu, Y.; Liu, Z.; Wang, J.; Conti, P. S.; Shi, X.; Chen, K., (64)Cu-Labeled multifunctional dendrimers for targeted tumor PET imaging. *Nanoscale* **2018,** 10, (13), 6113-6124.
28. Giri, J.; Diallo, M. S.; Simpson, A. J.; Liu, Y.; Goddard, W. A.; Kumar, R.; Woods, G. C., Interactions of poly(amidoamine) dendrimers with human serum albumin: binding constants and mechanisms. *ACS Nano* **2011,** 5, (5), 3456-68.
29. Neira, J. L.; Correa, J.; Rizzuti, B.; Santofimia-Castano, P.; Abian, O.; Velazquez-Campoy, A.; Fernandez-Megia, E.; Iovanna, J. L., Dendrimers as Competitors of Protein-Protein Interactions of the Intrinsically Disordered Nuclear Chromatin Protein NUPR1. *Biomacromolecules* **2019,** 20, (7), 2567-2576.
30. Curtis, R. A.; Ulrich, J.; Montaser, A.; Prausnitz, J. M.; Blanch, H. W., Protein-protein interactions in concentrated electrolyte solutions. *Biotechnol Bioeng* **2002,** 79, (4), 367-80.
31. Lin, Y. L.; Khanafer, K.; El-Sayed, M. E., Quantitative evaluation of the effect of poly(amidoamine) dendrimers on the porosity of epithelial monolayers. *Nanoscale* **2010,** 2, (5), 755-62.
32. Yang, B.; Xu, H.; Wang, S.; Cai, M.; Shi, Y.; Yang, G.; Wang, H.; Shan, Y., Studying the dynamic mechanism of transporting a single drug carrier-polyamidoamine dendrimer through cell membranes by force tracing. *Nanoscale* **2016,** 8, (42), 18027-18031.
33. Domenech, R.; Abian, O.; Bocanegra, R.; Correa, J.; Sousa-Herves, A.; Riguera, R.; Mateu, M. G.; Fernandez-Megia, E.; Velazquez-Campoy, A.; Neira, J. L., Dendrimers as potential inhibitors of the dimerization of the capsid protein of HIV-1. *Biomacromolecules* **2010,** 11, (8), 2069-78.

34. Pelaz, B.; del Pino, P.; Maffre, P.; Hartmann, R.; Gallego, M.; Rivera-Fernandez, S.; de la Fuente, J. M.; Nienhaus, G. U.; Parak, W. J., Surface Functionalization of Nanoparticles with Polyethylene Glycol: Effects on Protein Adsorption and Cellular Uptake. *ACS Nano* **2015,** 9, (7), 6996-7008.
35. Fahrlander, E.; Schelhaas, S.; Jacobs, A. H.; Langer, K., PEGylated human serum albumin (HSA) nanoparticles: preparation, characterization and quantification of the PEGylation extent. *Nanotechnology* **2015,** 26, (14), 145103.
36. Gon, S.; Santore, M. M., Sensitivity of protein adsorption to architectural variations in a protein-resistant polymer brush containing engineered nanoscale adhesive sites. *Langmuir* **2011,** 27, (24), 15083-91.
37. Alberio, T.; Colapinto, M.; Natale, M.; Ravizza, R.; Gariboldi, M. B.; Bucci, E. M.; Lopiano, L.; Fasano, M., Changes in the two-dimensional electrophoresis pattern of the Parkinson's disease related protein DJ-1 in human SH-SY5Y neuroblastoma cells after dopamine treatment. *IUBMB Life* **2010,** 62, (9), 688-92.
38. Alberio, T.; Lopiano, L.; Fasano, M., Cellular models to investigate biochemical pathways in Parkinson's disease. *Febs j* **2012,** 279, (7), 1146-55.
39. Faridi, A.; Yang, W.; Kelly, H. G.; Wang, C.; Faridi, P.; Purcell, A. W.; Davis, T. P.; Chen, P.; Kent, S. J.; Ke, P. C., Differential Roles of Plasma Protein Corona on Immune Cell Association and Cytokine Secretion of Oligomeric and Fibrillar Beta-Amyloid. *Biomacromolecules* **2019,** 20, (11), 4208-4217.
40. Ghadami, S. A.; Chia, S.; Ruggeri, F. S.; Meisl, G.; Bemporad, F.; Habchi, J.; Cascella, R.; Dobson, C. M.; Vendruscolo, M.; Knowles, T. P. J.; Chiti, F., Transthyretin Inhibits Primary and Secondary Nucleations of Amyloid-beta Peptide Aggregation and Reduces the Toxicity of Its Oligomers. *Biomacromolecules* **2020**.
41. Obeso, J. A.; Rodriguez-Oroz, M. C.; Goetz, C. G.; Marin, C.; Kordower, J. H.; Rodriguez, M.; Hirsch, E. C.; Farrer, M.; Schapira, A. H.; Halliday, G., Missing pieces in the Parkinson's disease puzzle. *Nat Med* **2010,** 16, (6), 653-61.
42. Roberts, D.; Keeling, R.; Tracka, M.; van der Walle, C. F.; Uddin, S.; Warwicker, J.; Curtis, R., Specific ion and buffer effects on protein-protein interactions of a monoclonal antibody. *Mol Pharm* **2015,** 12, (1), 179-93.
43. Delgado, A. V.; Gonzalez-Caballero, F.; Hunter, R. J.; Koopal, L. K.; Lyklema, J., Measurement and interpretation of electrokinetic phenomena. *J Colloid Interface Sci* **2007,** 309, (2), 194-224.
44. Lopes, F. M.; Schroder, R.; da Frota, M. L., Jr.; Zanotto-Filho, A.; Muller, C. B.; Pires, A. S.; Meurer, R. T.; Colpo, G. D.; Gelain, D. P.; Kapczinski, F.; Moreira, J. C.; Fernandes Mda, C.; Klamt, F., Comparison between proliferative and neuron-like SH-SY5Y cells as an in vitro model for Parkinson disease studies. *Brain Res* **2010,** 1337, 85-94.
45. Kovalevich, J.; Langford, D., Considerations for the use of SH-SY5Y neuroblastoma cells in neurobiology. *Methods Mol Biol* **2013,** 1078, 9-21.
46. Cheung, Y. T.; Lau, W. K.; Yu, M. S.; Lai, C. S.; Yeung, S. C.; So, K. F.; Chang, R. C., Effects of all-trans-retinoic acid on human SH-SY5Y neuroblastoma as in vitro model in neurotoxicity research.

Neurotoxicology **2009,** 30, (1), 127-35.

47. Mohammadniaei, M.; Yoon, J.; Choi, H. K.; Placide, V.; Bharate, B. G.; Lee, T.; Choi, J. W., Multifunctional Nanobiohybrid Material Composed of Ag@Bi2Se3/RNA Three-Way Junction/miRNA/Retinoic Acid for Neuroblastoma Differentiation. *ACS Appl Mater Interfaces* **2019,** 11, (9), 8779-8788.
48. Beal, M. F., Experimental models of Parkinson's disease. *Nat Rev Neurosci* **2001,** 2, (5), 325-34.

Figures

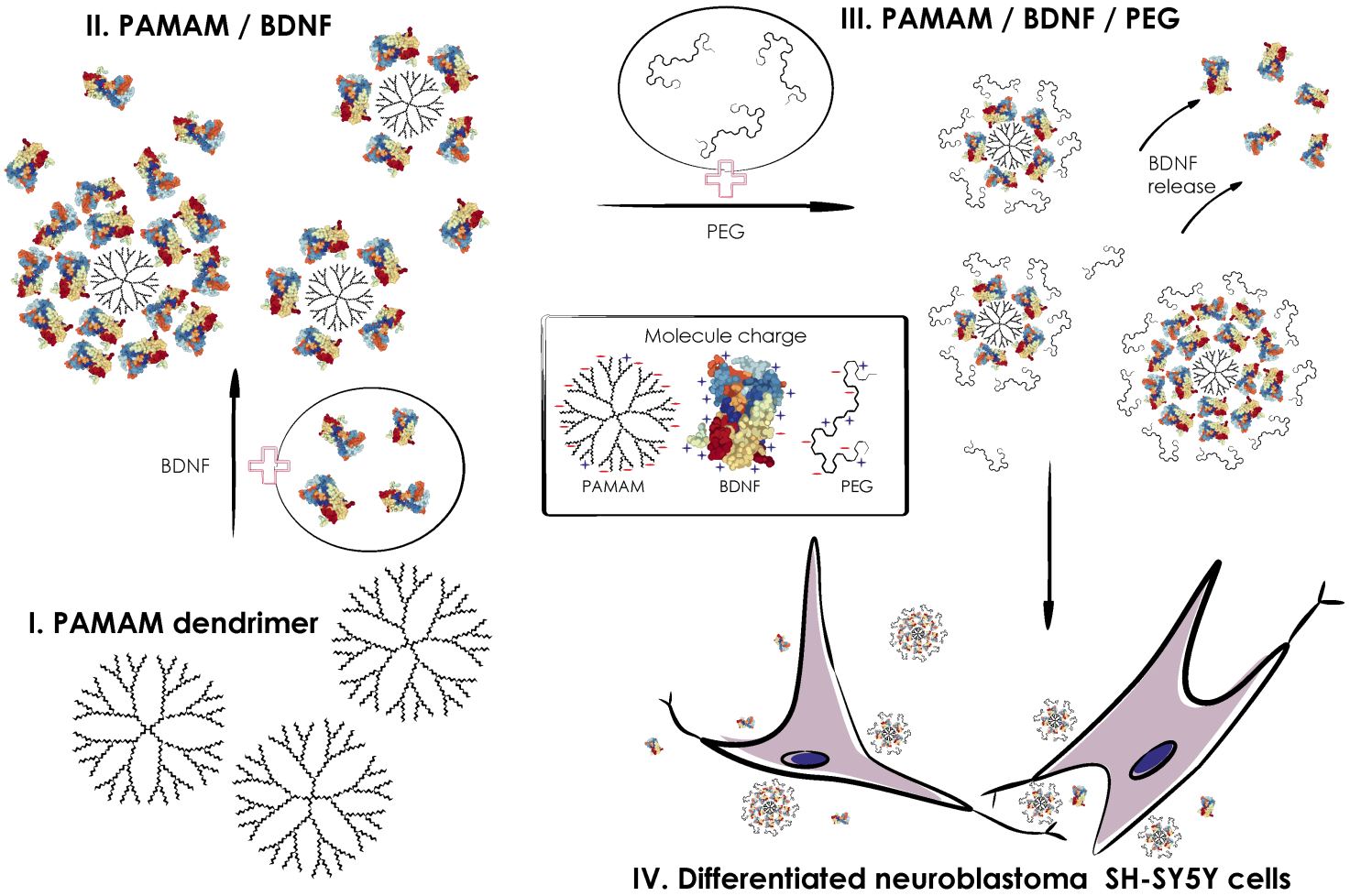

Figure 1

Schematic drawing of synthesis process of PEG-ylated BDNF-PAMAM dendrimer nanoparticles as well as BDNF delivery in differentiated neuroblastoma SH-SY5Y cells. Inserted frame comprises molecular structures of BDNF protein, PAMAM and PEG polymer molecules with their overall charge at pH 7.4.

a)

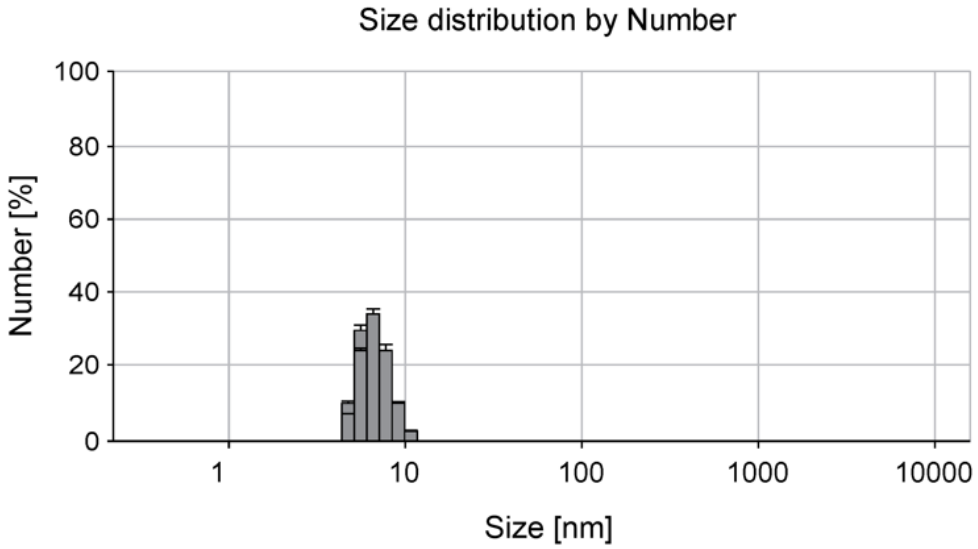

b)

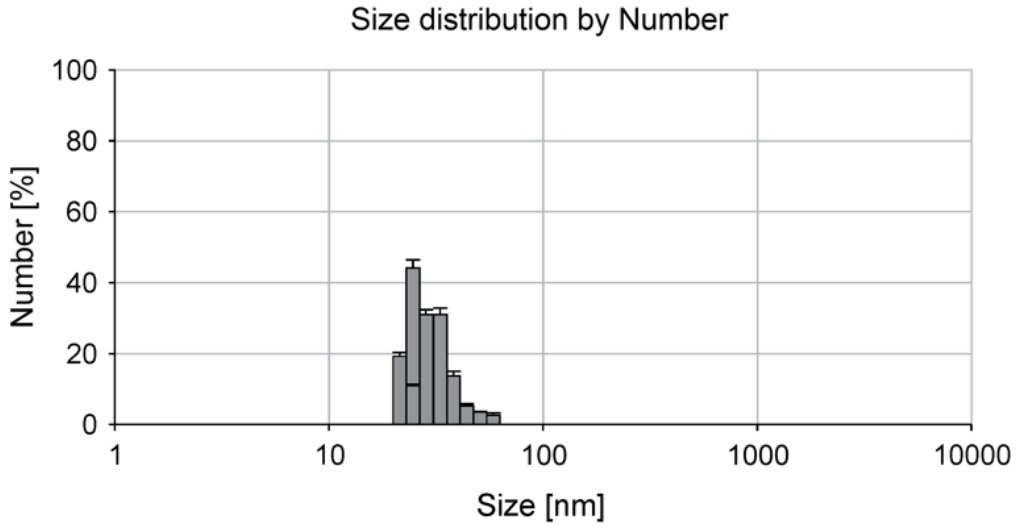

Figure 2

Typical size distribution of BDNF-PAMAM (a) and PEG-ylated BDNF-PAMAM (b) nanoparticles measured in the bulk by DLS (0.15 M PBS, pH 7.4) without an ultrafiltration process. All values are representative of 5 independent experiments and are expressed as mean +/- SD.

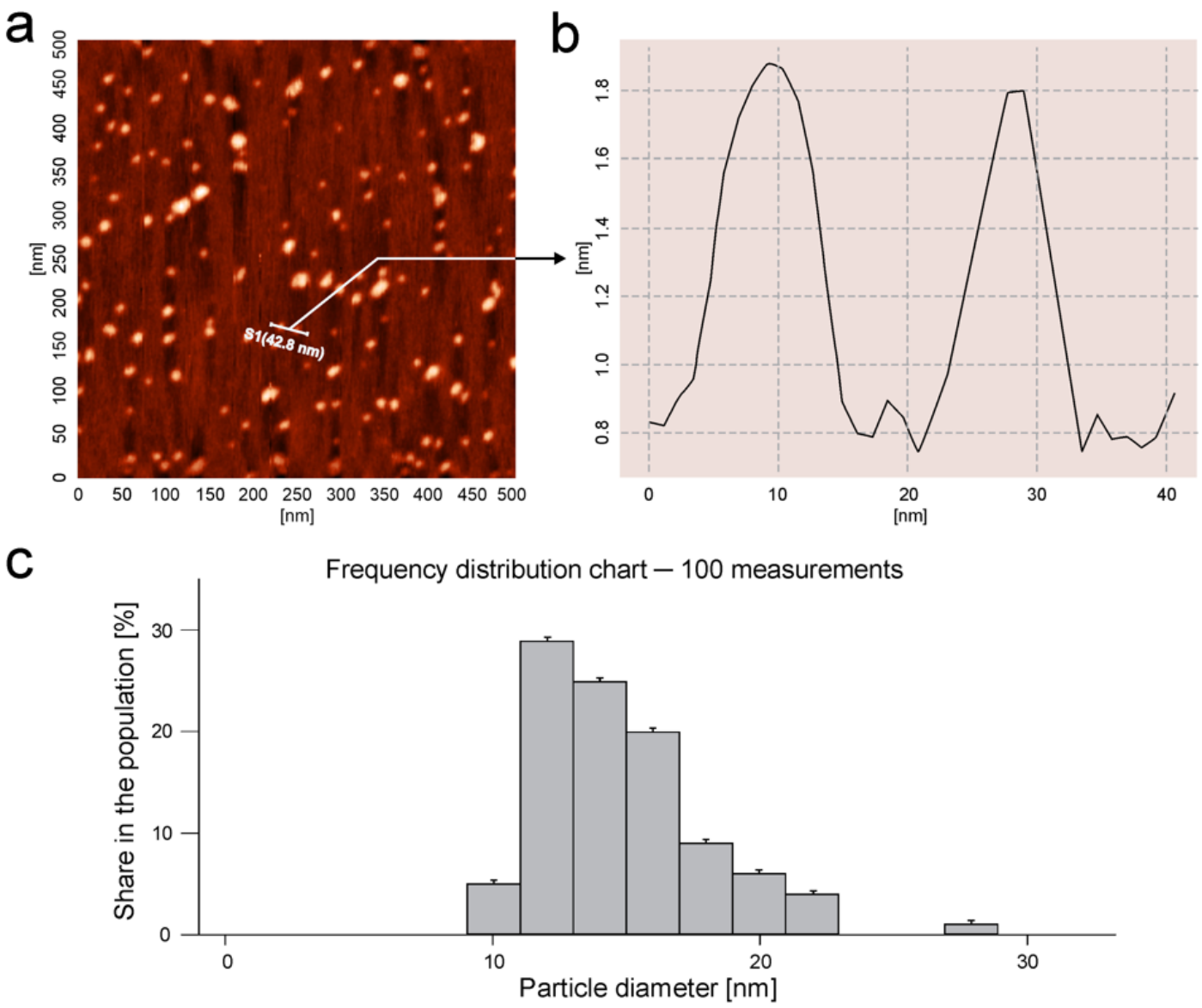

Figure 3

AFM analysis of PAMAM-BDNF (above part) and PEG-ylated PAMAM-BDNF (below part) nanoparticles adsorbed at mica surface at 0.15M pH 7.4: PBS. a Scan of PAMAM-based nanoparticles at scan area 0.5 x 05 μm. b Structure of PAMAM-based nanoparticles after cross-section. c Histogram of adsorbed nanoparticles indicated by direct AFM enumeration, obtained for low surface molecules concentration. The Figure was created by taking into account 10 randomly chosen areas, where each micrograph of PAMAM-based monolayer at the mica surface has a size of 0.5 x 05 μm.

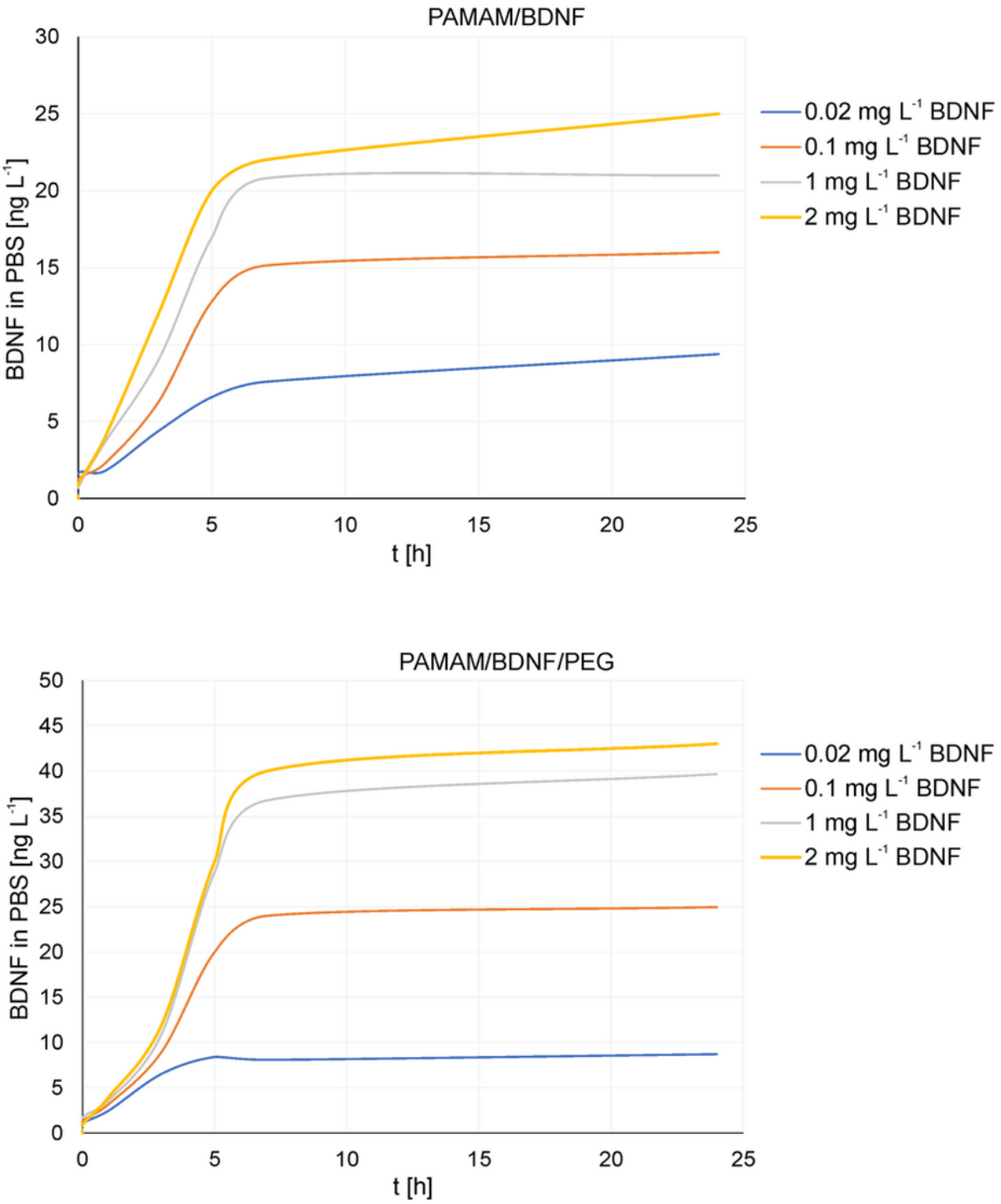

Figure 4

Desorption characteristic of BDNF from PAMAM G5.5 dendrimers-based nanoparticles in PBS electrolyte with increasing loading of protein concentrations from 0.02 to 1 mg L-1. BDNF detection by ELISA over 24 h of incubation (a) PAMAM-BDNF and (b) PEG-ylated PAMAM-BDNF nanoparticles.

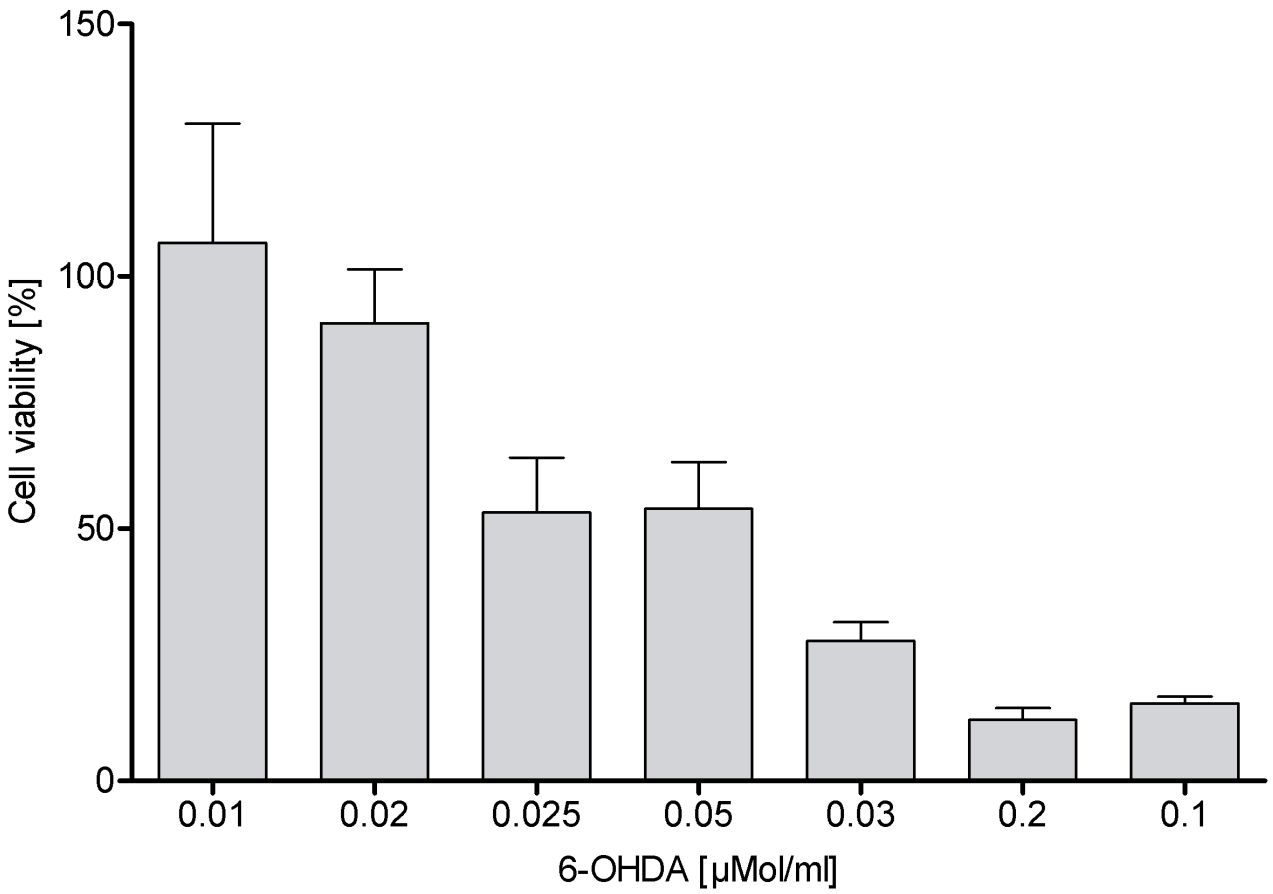

Figure 5

Cytotoxicity curves for 6-OHDA. Differences in sensitivity of differentiated human neuroblastoma cell line SH-SY5Y to the 6-OHDA neurotoxin. The data represent means +/- SD for 30 experiments.

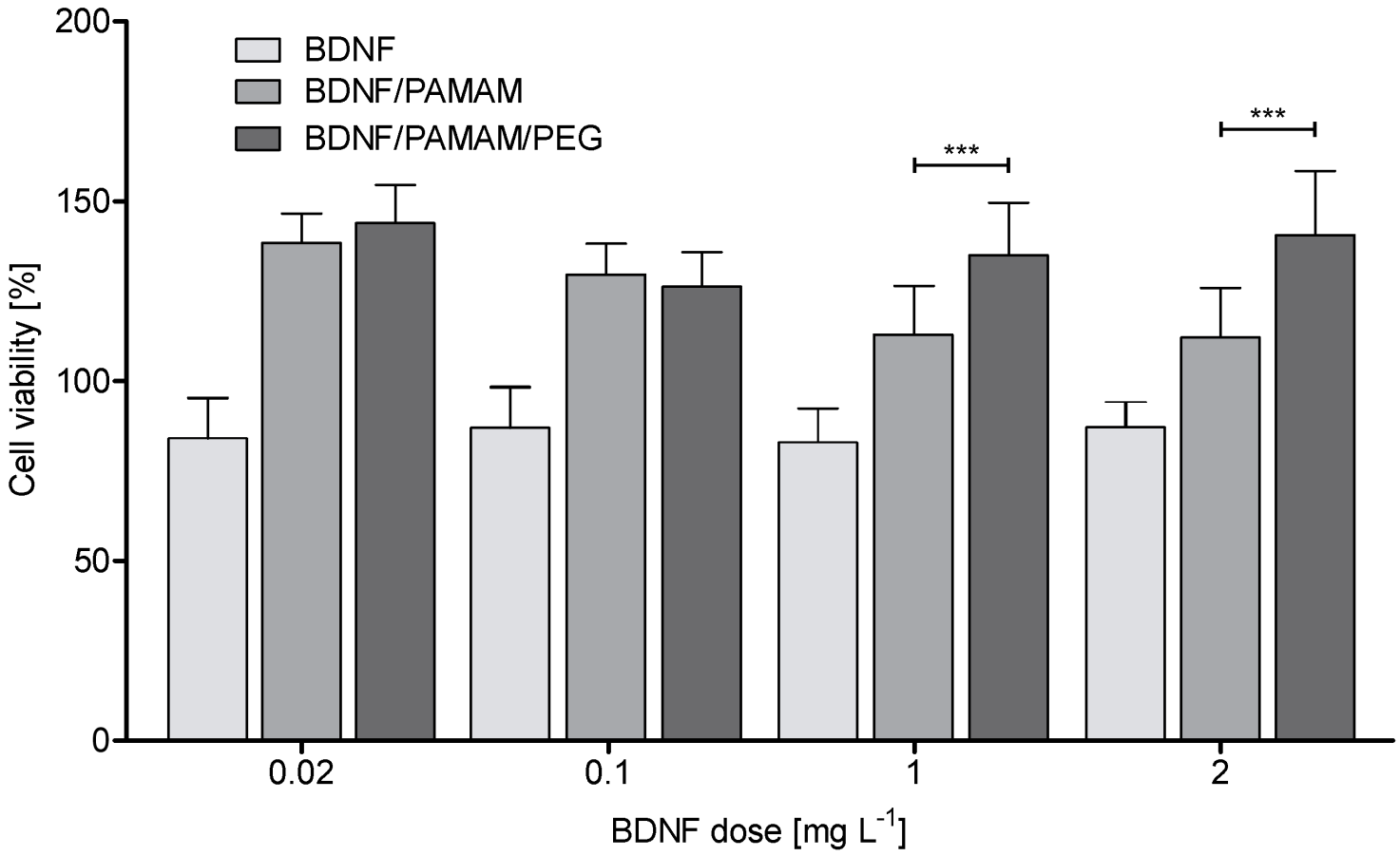

Figure 6

Cytotoxicity curves for BDNF, PAMAM-BDNF and PEG-ylated PAMAM-BDNF nanoparticles in differentiated human neuroblastoma cell line SH-SY5Y treated with the 100 μMol/L 6-OHDA neurotoxin. The data represent means +/- SD for 30 experiments.

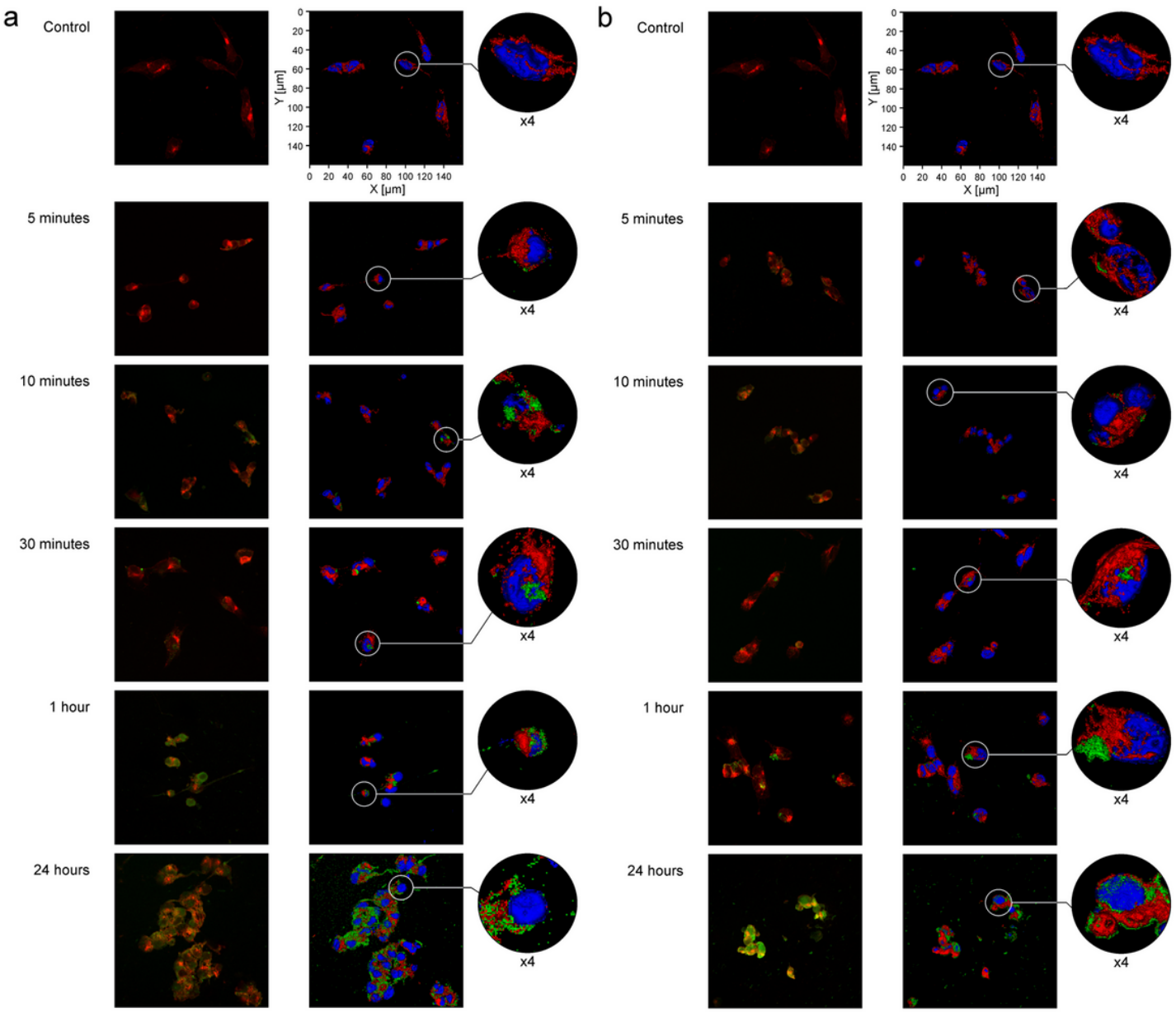

Figure 7

Cellular internalization of PAMAM-based nanoparticles by neuron-like differentiated human neuroblastoma SH-SY5Y cell. The cells were incubated either with BDNF-PAMAM-AF488 (part a) or BDNF-PAMAM-AF488-PEG (part b) nanoparticles (green color) for different time lengths (5min, 10min, 30min, 1h and 24h) and then co-stained with WGA-Texas Red-X (red) and DAPI (blue). Confocal fluorescence images on the right panel are render series of z-stack with applied surface mode. Panel on the left presents single stack from the z-stack and only nanoparticles (green) and surface glycoproteins (red) are shown. The images were taken at 400x magnification.

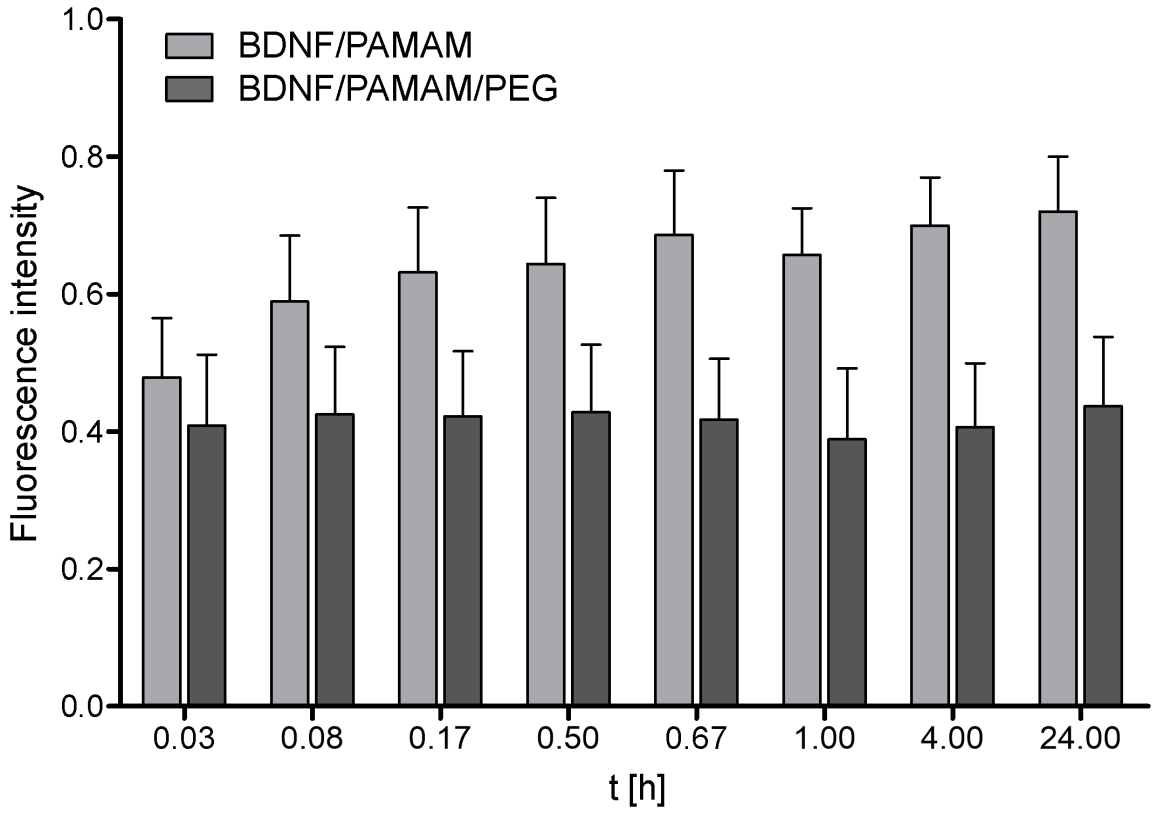

Figure 8

Immunofluorescence assessment of dendrimers-based nanoparticles internalization by neuron-like differentiated human neuroblastoma cell line SH-SY5Y upon treatment for 0, 2-60min, 4h and 24h. Data were presented as the mean +/- SD (n = 12).

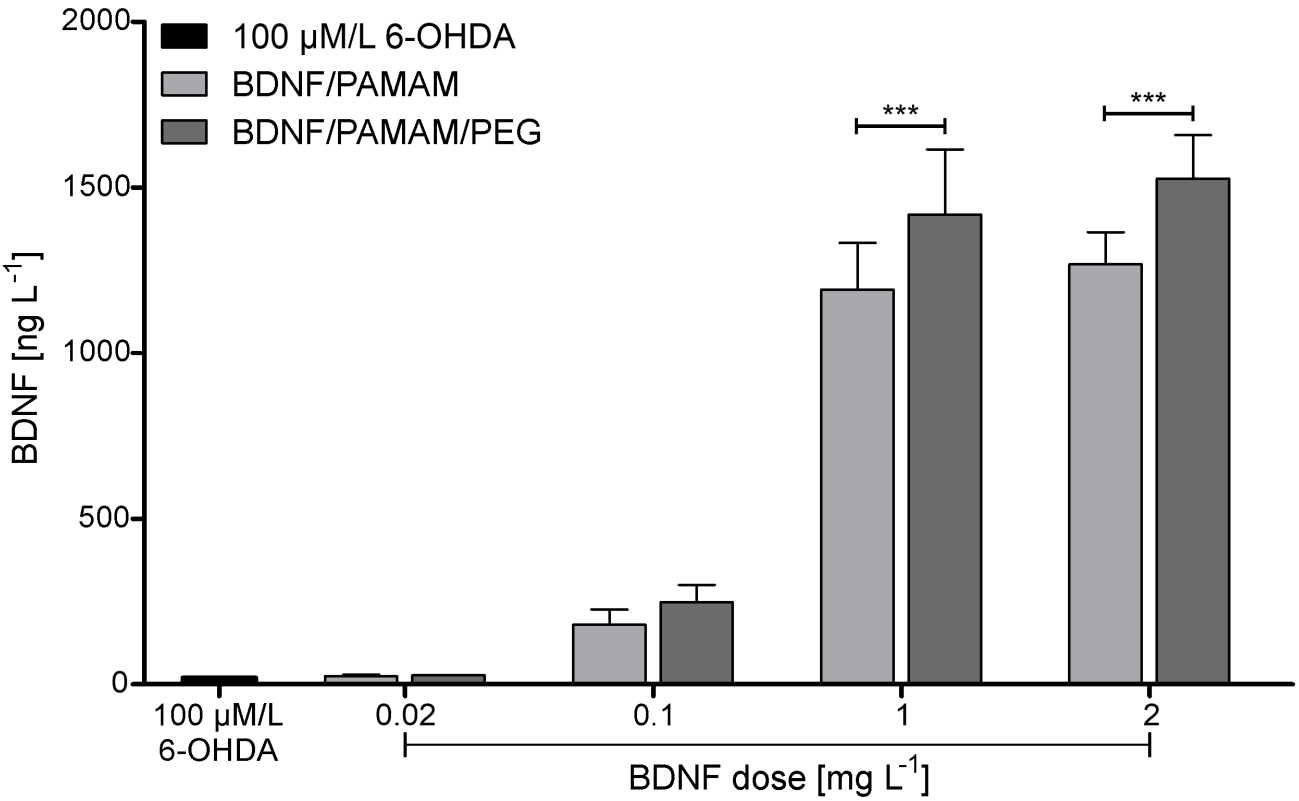

Figure 9

Desorption characteristic of BDNF from PAMAM G5.5 dendrimers-based nanoparticles for neuron-like differentiated human neuroblastoma cell line SH-SY5Y under increasing nanocarriers loading of protein concentrations from 0.02 to 2 mg L-1. BDNF detection by ELISA over 24 h of incubation cells with BDNF proteins, PAMAM-BDNF nanoparticles and PEG-ylated PAMAM-BDNF nanoparticles. The data represent means +/- SD for five experiments.

Supplementary Files

This is a list of supplementary files associated with this preprint. Click to download.

- TOC.tif
- BDNFSupportingInfo21march.docx